Neuron, Vol. 18, 411–423, March, 1997, Copyright ©1997 by Cell Press

Defects in Sensory and Autonomic Ganglia and Absence of Locus Coeruleus in Mice Deficient for the Homeobox Gene *Phox2a*

Xavier Morin,*‡ Harold Cremer,*‡ Marie-Rose Hirsch,* Raj P. Kapur,† Christo Goridis,* and Jean-François Brunet*§

*Laboratoire de Génétique et Physiologie du Développement
Institut de Biologie du Développement de Marseille
CNRS/INSERM/Université de la Méditerranée
Marseille
France

†Department of Pathology
Children's Hospital and Medical Center
Seattle, Washington 98105

Summary

Phox2a is a vertebrate homeodomain protein expressed in subsets of differentiating neurons. Here, we show that it is essential for proper development of the locus coeruleus, a subset of sympathetic and parasympathetic ganglia and the VIIth, IXth, and Xth cranial sensory ganglia. In the sensory ganglia, we have identified two differentiation blocks in *Phox2a*$^{-/-}$ mice. First, the transient expression of dopamine-β-hydroxylase in neuroblasts is abolished, providing evidence that Phox2a controls noradrenergic traits in vivo. Second, the expression of the GDNF receptor subunit Ret is dramatically reduced, and there is a massive increase in apoptosis of ganglion cells, which are known to depend on GDNF in vivo. Therefore, Phox2a appears to regulate conventional differentiation traits and the ability of neurons to respond to essential survival factors.

Introduction

Transcription factors provide probably the best markers for the molecular description of the histogenesis of the vertebrate nervous system. In the central nervous system, some of them define broad domains of the proliferative neuroepithelium before any morphological landmark is visible and are therefore thought to specify regions of the nervous system. Others are selectively expressed in classes of neurons or neuroblasts and may therefore control later stages of differentiation (reviewed by Rubenstein and Puelles, 1994; Bang and Goulding, 1996). However, their precise role in neuronal (or regional) specification has been difficult to analyse genetically.

In invertebrates, gain- or loss-of-function mutations of neuron-specific transcription factors often result in fate switches, providing a first insight in what part of the differentiation pathway they control. In Drosophila, for example, the homeodomain protein Cut, expressed in sensory organ precursors, behaves like a "master switch" between two sensory organ identities: external sensory organs and chordotonal organs (reviewed by Ghysen and Dambly-Chaudière, 1993). Similarly, the level of expression of the homeodomain proteins BarH1 and BarH2 commits the development of external sensory organs to particular subtypes (Higashijima et al., 1992). In the nematode C. elegans, the homeoprotein Unc-4, expressed in a defined motoneuron, determines which of two interneurons will synapse on it (Miller et al., 1992; Miller and Niemeyer, 1995).

In vertebrates, by contrast, inactivation of transcriptional regulators of neural development has mainly resulted in the atrophy or deletion of part of their expression domains, often hampering a phenotypic analysis of the mutations at the cellular level (for examples, see Nakai et al., 1995; Schonemann et al., 1995; Erkman et al., 1996; Gan et al., 1996; Kimura et al., 1996; Pfaff et al., 1996). Some clues about the precise role of various transcription factors in neuronal differentiation have come from correlative evidence. One of the most striking examples to date is the remarkable correlation between the set of LIM-type homeodomain proteins expressed by a spinal motoneuron and the class of muscle it innervates (Tsuchida et al., 1994; Appel et al., 1995).

Phox2 (now renamed Phox2a, see below) is a homeodomain protein whose expression pattern is limited to sets of differentiating neurons (Valarché et al., 1993; Tiveron et al., 1996): all ganglia of the peripheral autonomic nervous system; the distal, placode-derived components of the VIIth, IXth, and Xth cranial sensory ganglia (the geniculate, petrose, and nodose ganglia, respectively); and some hindbrain nuclei, including all noradrenergic centers. One striking correlate that emerges from the survey of Phox2a expression sites is that Phox2a is expressed in all neurons that, permanently or transiently, express features of the (nor)adrenergic phenotype, and, in particular, the last enzyme of the norepinephrine synthesis pathway, dopamine-β-hydroxylase (DBH) (Valarché et al., 1993; Tiveron et al., 1996). We recently isolated a closely related protein, Phox2b, with an identical homeodomain, expressed in a very similar but distinct pattern (A. Pattyn, X. M., C. G., and J. F. B., unpublished data).

To determine the role of Phox2a, we generated mice with a null mutation in the *Phox2a* gene. We find that *Phox2a*$^{-/-}$ mice completely lack a locus coeruleus (l.c.), the main noradrenergic center of the brain. Furthermore, parasympathetic ganglia in the head are missing, and the superior cervical ganglion as well as cranial sensory ganglia that normally express Phox2a are severely affected. Moreover, we show that the affected sensory ganglia fail to express *DBH* transiently as they normally do, providing in vivo evidence that Phox2a is a determinant of the noradrenergic phenotype. We also show that they fail, for the most part, to express Ret, a receptor subunit for the glial cell–derived neurotrophic factor (GDNF) on which they are known to depend in vivo (Moore et al., 1996). Therefore, Phox2a appears to coregulate classical differentiation features of some neurons (like their neurotransmitter phenotype), as well as

‡These authors contributed equally to this work.

§Address correspondence to: Dr. J.-F. Brunet, IBDM, Campus de Luminy, case 907, F-13288 Marseille Cedex 9, France.

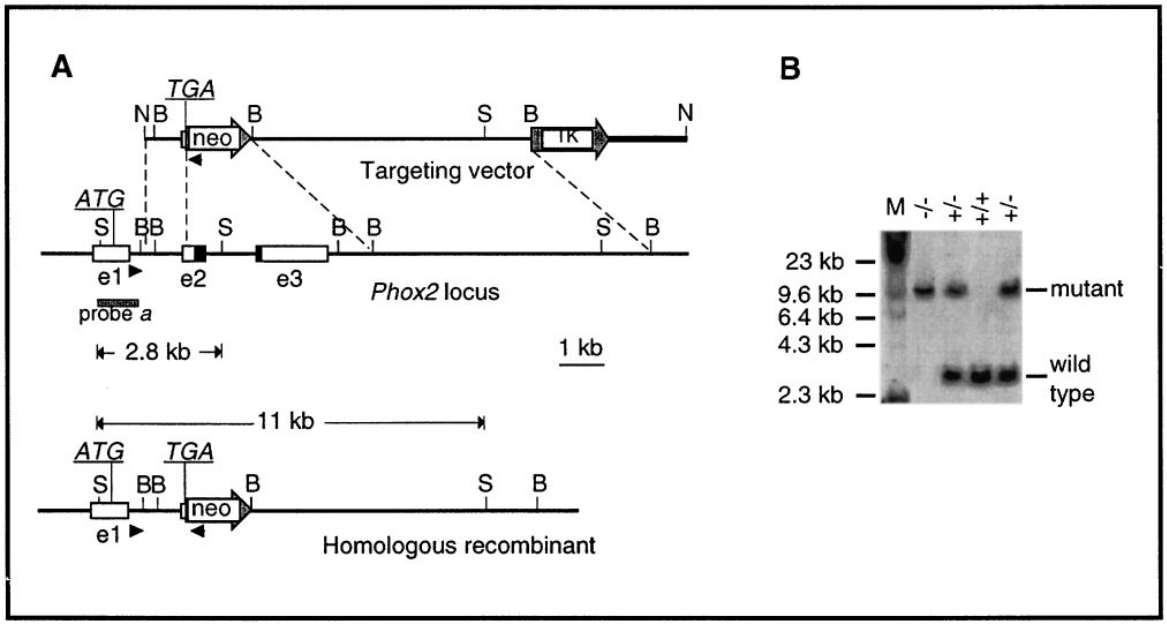

Figure 1. Generation of *Phox2a*$^{-/-}$ Mice

(A) Representation of the targeting vector pΔPhox2a (top), the wild-type mouse *Phox2a* locus (middle), and the expected recombinant allele (bottom). Open boxes represent exons. The homeodomain is indicated in black. Arrowheads indicate oligonucleotides used for PCR screening of recombinant ES cells. The expected sizes of the SstI fragments from the wild-type and the mutant loci hybridizing to probe *a* are indicated. B, BamHI; S, SstI; and N, NotI.

(B) Southern blot analysis of tail DNA from wild-type, heterozygous, and homozygous littermates showing correct targeting of the *Phox2a* locus. DNA samples were digested with SstI and hybridized with probe *a* (M, size markers).

their capacity to respond to essential trophic factors, thereby establishing a direct link between neuronal identity and survival.

Results

We created a null mutation in the mouse *Phox2a* gene by deleting the homeobox and all coding sequences downstream (Figure 1A). The homeodomain is essential to the function of homeodomain proteins, and homeobox deletions have been shown to behave like null mutants of homeobox genes (e.g., Goddard et al., 1996). Correctly targeted embryonic stem (ES) cells were identified by polymerase chain reaction (PCR) analysis, confirmed by genomic Southern analysis, and injected into C57BL/6 host blastocysts to generate chimeric mice. Germ-line transmission was obtained with two independent clones, which gave rise to similar phenotypes. Mice hemizygous for the mutant allele did not show an obvious phenotype and bred normally. Mice homozygous for the mutation were born in roughly Mendelian proportions. They were of normal size, without gross anatomical anomaly, and appeared to breathe normally, but they did not feed and died on the day of birth. Immunohistochemistry with an anti-Phox2a antiserum (directed against the C-terminus of the protein) did not give any signal, thereby confirming the correct targeting of the locus (not shown). We cannot formally exclude that the isolated NH2 terminal peptide performs a function in mutant embryos. However, a 5′ *Phox2a* cRNA probe, corresponding to the residual coding sequences in the mutant locus, which revealed the normal pattern of *Phox2a* expression in wild-type and heterozygous animals, did not give any signals on homozygous mutants (not shown), arguing that the truncated message, presumably unstable, is unlikely to contribute any phenotype.

Defects in Autonomic Ganglia

We examined the three divisions of the peripheral autonomic nervous system, which normally express Phox2a (Valarché et al., 1993; Tiveron et al., 1996): parasympathetic, sympathetic, and enteric.

Parasympathetic Ganglia

The parasympathetic ganglia of the head were examined at birth by conventional histological staining. The otic ganglion, normally in close apposition to the pterygopalatine artery (Figure 2A), was missing in *Phox2a*$^{-/-}$ mutants (Figure 2B). The sphenopalatine ganglion, which appears as an elongated group of cells along the maxillary branch of the trigeminal nerve, was also absent in the mutants (not shown). At midgestation, neither the otic nor the sphenopalatine ganglia were detectable by in situ hybridization for the panneuronal marker *Ncam* (Figures 2C and 2D, and not shown), and the absence of the cells was evident by Nomarski optics (not shown). In contrast, the submandibular complex, as visualized by in situ hybridization for *Ncam*, was only partially affected, with variable penetrance (not shown). The paracardiac ganglia, which are the caudalmost identifiable ganglia, appeared normal (Figures 2E and 2F). Thus, there is a rostrocaudal gradient in the degree to which parasympathetic ganglia depend on Phox2a.

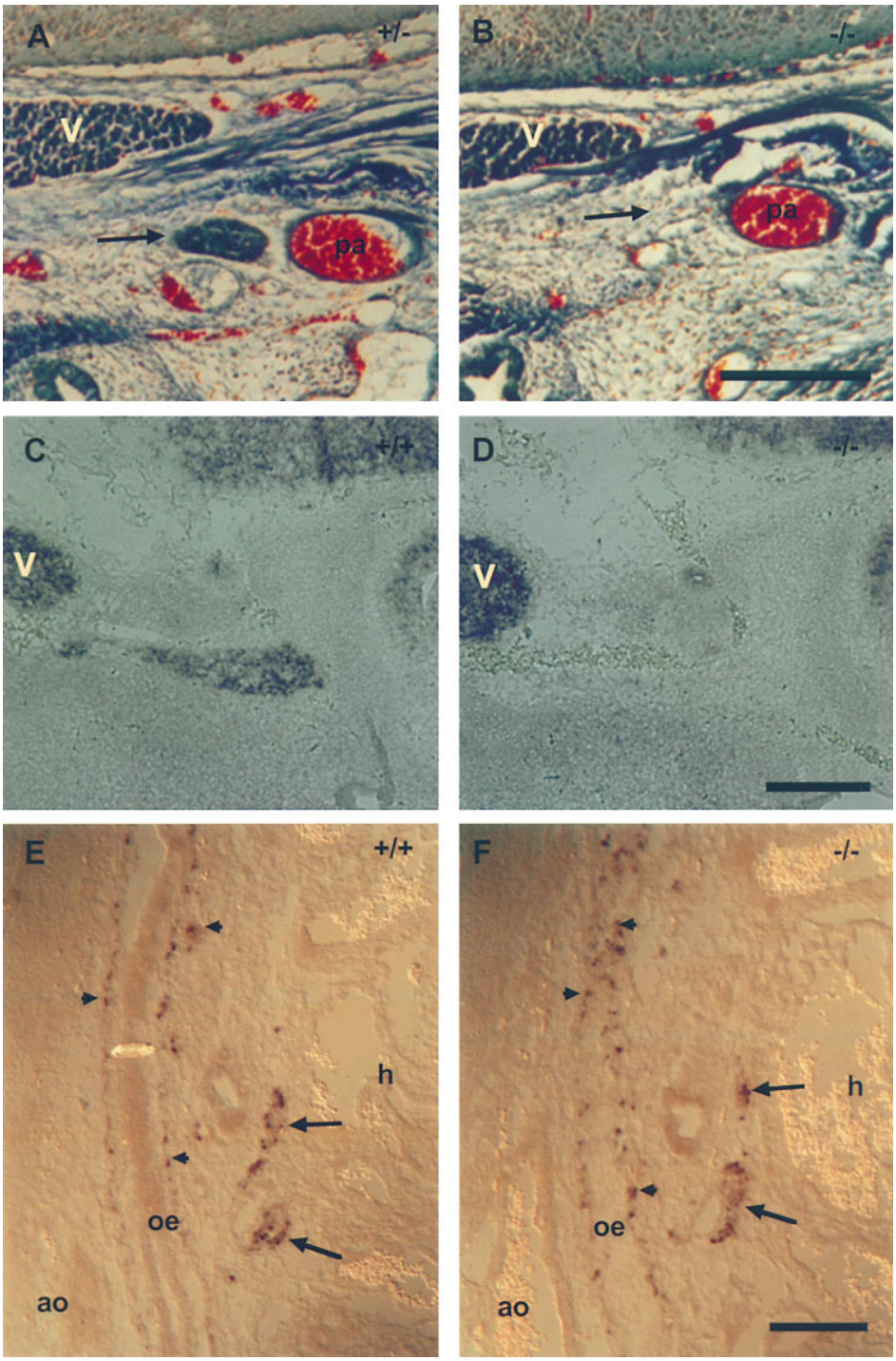

Figure 2. Absence of the Rostral Parasympathetic Ganglia in *Phox2a*$^{-/-}$ Mice

(A and B) Histological staining of parasagittal sections of the head of newborn mice. The otic ganglion (arrows), in close apposition to the pterygopalatine artery (A), is missing in the mutants (B).

(C and D) In situ hybridization with an *Ncam* probe on parasagittal sections at E13.5: the sphenopalatine ganglion, appearing as an elongated group of *Ncam*$^{+}$ cells along the maxillary branch of the trigeminal nerve (C), is absent in *Phox2a* mutants (D).

(E and F) In situ hybridization with a *Ret* probe on parasagittal sections at E13.5 do not reveal any defect in the paracardiac ganglia (arrows) of the mutants (F) compared to control mice (E). Note that the ganglia along the esophagus (arrowheads), which normally express Phox2a, seem also unaffected by the mutation. a, aorta; h, heart; oe, esophagus; pa, pterygopalatine artery; and V, trigeminal ganglion. Scale bars = 500 μm, (A) and (B); 200 μm, (C–F).

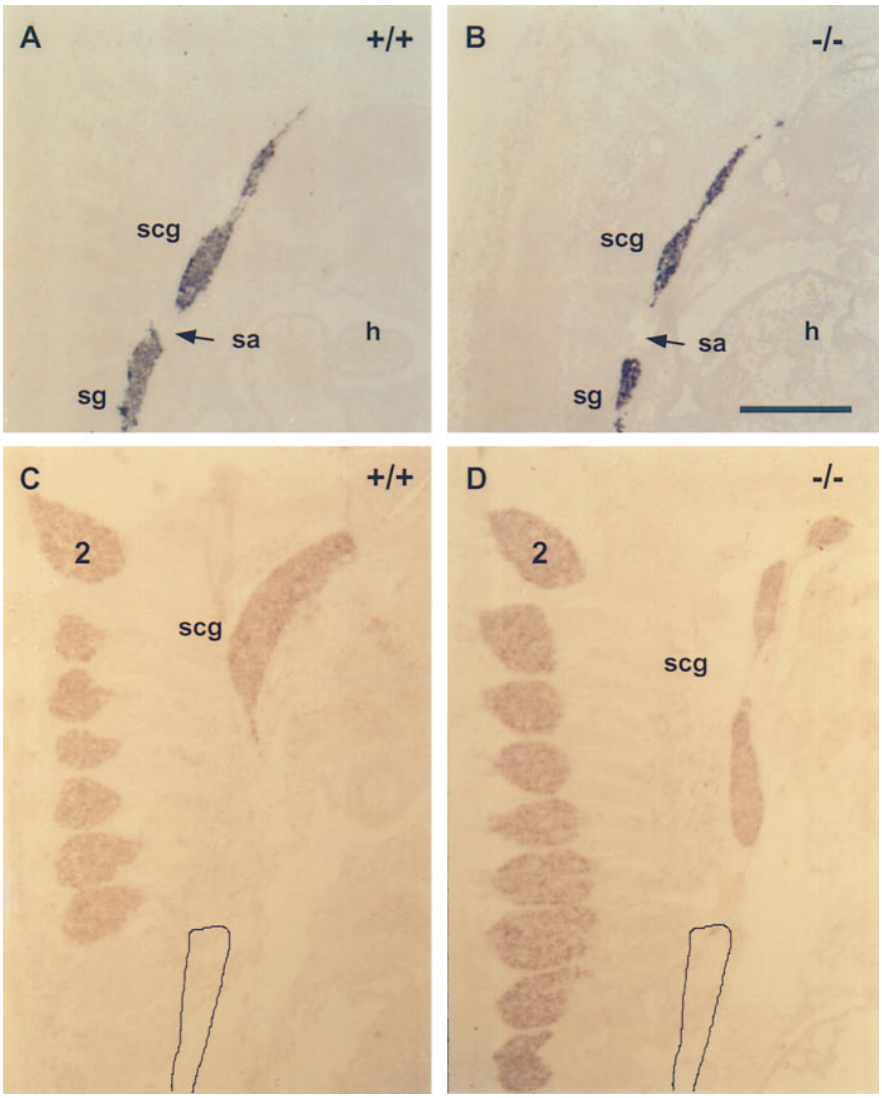

Figure 3. Morphological Defect of the Superior Cervical Ganglion in *Phox2a*$^{-/-}$ Mice

(A and B) In situ hybridization with a *DBH* probe on parasagittal sections of E11.5 mice does not reveal any difference at the level of the SCG between control (A) and mutant (B) mice. At this stage, the sympathetic chain consists in a column of *DBH*$^{+}$ cells extending rostrally up to the level of vertebra C4 with a small gap (arrows) created by the subclavicular artery separating the cervical and thoracic levels.

(C and D) At E13.5, in situ hybridization with an *Ncam* probe reveals a defect in the morphology of the SCG: in wild-type mice, it is a large fusiform ganglion whose rostral pole abuts the cochlea and whose caudal pole is in register with the 4th cervical vertebra (C). By contrast, in *Phox2a*$^{-/-}$ mice, the SCG is smaller, with an exaggerated constriction, which makes it appear split in many section planes. In addition, a second cervical ganglion is present, lying more caudally, still close to the stellate ganglion. The position of the stellate ganglion, seen on adjacent sections, is outlined. 2, dorsal root ganglion of C2; h, heart; sa, subclavicular artery; scg, superior cervical ganglion; sg, stellate ganglion. Scale bar = 200 μm.

Sympathetic Ganglia

Phox2a is normally expressed in the sympathoadrenal lineage of the neural crest, as soon as these cells aggregate next to the dorsal aorta to form the primary sympathetic chain and concomitantly with their expression of *tyrosine hydroxylase* message (*TH*) and *DBH* (Valarché et al., 1993; Ernsberger et al., 1995; Tiveron et al., 1996). This expression persists throughout embryogenesis and into postnatal stages. The early differentiation of the sympathetic chain, as monitored by in situ hybridization for *Ncam*, *Ret*, *TH*, or *DBH*, was not visibly affected in *Phox2a*$^{-/-}$ embryos (Figures 3A and 3B, and not shown). Until E11.5, the sympathetic chain of wild-type and mutant mice consists of a column of *DBH*$^{+}$ cells extending rostrally up to the level of vertebra C4 (Figures 3A and 3B). Two days later, in wild-type mice, the levels from C7–C3 are devoid of *DBH*$^{+}$ cells, while at the level of C1–C3, the superior cervical ganglion (SCG) has now formed (Figure 3C). This morphogenetic sequence has been attributed to a rostral migration of sympathetic cells from the lower cervical level, which is eventually completely depleted (Rubin, 1985). In *Phox2a*$^{-/-}$ E13.5 embryos, the SCG was smaller (Figure 3D) and, in all embryos examined (four/four), a second cervical gan-

Table 1. Neuronal Counts in Peripheral Sensory and Sympathetic Ganglia of Wild-Type and *Phox2a* Mutant Newborn Mice

	Wild-Type mean ± sem (n)	Phox2a Mutant mean ± sem (n)	Reduction (%)
Sensory ganglia			
Petrose-nodose	7305 ± 368 (n = 3)	1686 ± 387 (n = 3)	77%*
Superior-jugular	2623 ± 254 (n = 3)	2761 ± 115 (n = 3)	n.s.
Geniculate	1678 ± 53 (n = 3)	928 ± 122 (n = 3)	45%**
Sympathetic ganglia			
Superior cervical	31945 ± 1957 (n = 3)	27490 ± 2235 (n = 3)	n.s.
Stellate	20603 ± 1518 (n = 3)	21491 ± 2792 (n = 2)	n.s.

The cervical region of newborn mice was sectioned at 12 μm. Neurons with a clear nucleus were counted in every fifth section (see Experimental Procedures). The values were not corrected for split nuclei. Student's T test: *$p < 0.001$, **$p < 0.02$.

glion was present, lying ventral to vertebrae C4–C6, close to the stellate ganglion, which appeared normal. This is most simply explained by the formation of a new "intermediate" ganglion, at the expense of the SCG, through a deficit in rostral cell migration. No other morphological anomaly was observed in the rest of the sympathetic system, including the adrenal medulla. *DBH* and *TH* expression was unaffected in all of these structures until E13.5, the last stage examined (Figures 3A, 3B, and not shown). The morphological anomaly of the SCG persisted at birth (not shown). However, the size of the cervical complex, including the intermediate ganglion, was not significantly different from that of the wild-type SCG (Table 1).

Finally, we examined the myenteric plexus of *Phox2a*$^{-/-}$ embryos, using *Ncam* and *Ret* as probes but could not detect any obvious anomaly (Figures 2E, 2F, and not shown).

In summary, Phox2a is expressed in all ganglionic neurons of the peripheral autonomic system but seems necessary for the proper development of only a subset of sympathetic and parasympathetic ganglia.

Absence of the Locus Coeruleus in *Phox2a*$^{-/-}$ Mice

We then examined the central nervous system of mutant neonates after histological staining. The l.c., easily detectable on histologically stained coronal sections through the pons of wild-type mice as a compact group of large, darkly stained neurons in the lateral floor of the fourth ventricle (Figure 4A), was conspicuously absent in the brain stem of neonate mutant mice (Figure 4B). Complete lack of the l.c. was confirmed by in situ hybridization for *DBH* (Figures 4C and 4D). Surprisingly, other (nor)adrenergic areas, including the locus subcoeruleus and areas A1–C1, A2–C2, and A5, were apparently spared and expressed *DBH* (see Figures 4C and 4D for the locus subcoeruleus; others not shown). The status of the l.c. was assessed at different stages of embryogenesis by in situ hybridization with a *DBH* probe. In E13.5 wild-type mice, it is detectable as a characteristically shaped column of *DBH*$^{+}$ cells in the floor of the fourth ventricle (Figure 4E). No signal was detected in *Phox2a*$^{-/-}$ mice, save for scattered *DBH*$^{+}$ cells in the locus subcoeruleus region (Figure 4F). There was also no detectable expression of *TH* in the l.c. proper (not shown). Whole-mount in situ hybridization with a *DBH* probe confirmed this finding at E10.5, the earliest time point at which the l.c. anlage is visible with this marker (Figures 4G and 4H). These results establish that the noradrenergic cells of the l.c. depend on Phox2a for proper differentiation and/or survival.

Another hindbrain nucleus that expresses Phox2a, the facial motor nucleus (Tiveron et al., 1996), could be identified in the mutants by histological staining and appeared normal (not shown).

Atrophy of Cranial Sensory Ganglia

Formation of the distal VIIth, IXth, and Xth ganglia starts between E9.0 and E9.5, when neuronal progenitors delaminate from the epibranchial placodes and migrate toward the neural tube where they aggregate to form the ganglion primordia. At this stage, Phox2a is already prominently expressed in the placodes, the delaminating neuroblasts, and the forming ganglia. Phox2a expression persists through midgestation but gradually disappears thereafter (Valarché et al., 1993; Tiveron et al., 1996). In mutant neonates, the distal ganglionic complex of the IXth and Xth cranial nerves (petrose and nodose ganglia) was severely atrophic (Figures 5A and 5B), whereas the proximal neural crest–derived part of these ganglia (the superior–jugular complex), which does not normally express Phox2a, was unaffected. Neuronal counts in the IXth and Xth distal ganglia revealed a 77% cell loss in newborn mutant animals (Table 1). The distal (geniculate) ganglion of the VIIth nerve was also affected, albeit to a lesser extent (45% loss of neurons) (Table 1).

Homozygous mutant embryos were analyzed to determine the stage at which the development of these ganglia was disrupted. Already at E13.5, the nodose–petrose ganglionic complex was visibly reduced in size as assessed by in situ hybridization with an *Ncam* probe (Figures 5C and 5D). At earlier stages, *Ncam* was weakly expressed even in wild-type embryos and could not be used as probe. We thus used immunohistochemistry with antibodies to Class III β-tubulin, a very early marker of differentiating neurons (Easter et al., 1993), to visualize the ganglion anlagen at E10.5. No difference was visible between mutant and control embryos at this stage (Figures 5E and 5F). We also used as a marker the *lacZ* gene driven by a fragment of the human *DBH* promoter (Kapur et al., 1991; Mercer et al., 1991), a convenient early marker for all cranial sensory neurons (Kapur et al., 1991) whose expression is unaffected by the *Phox2a* mutation. Whole-mount preparations of E10.5 embryos harboring the *DBH-lacZ* transgene and

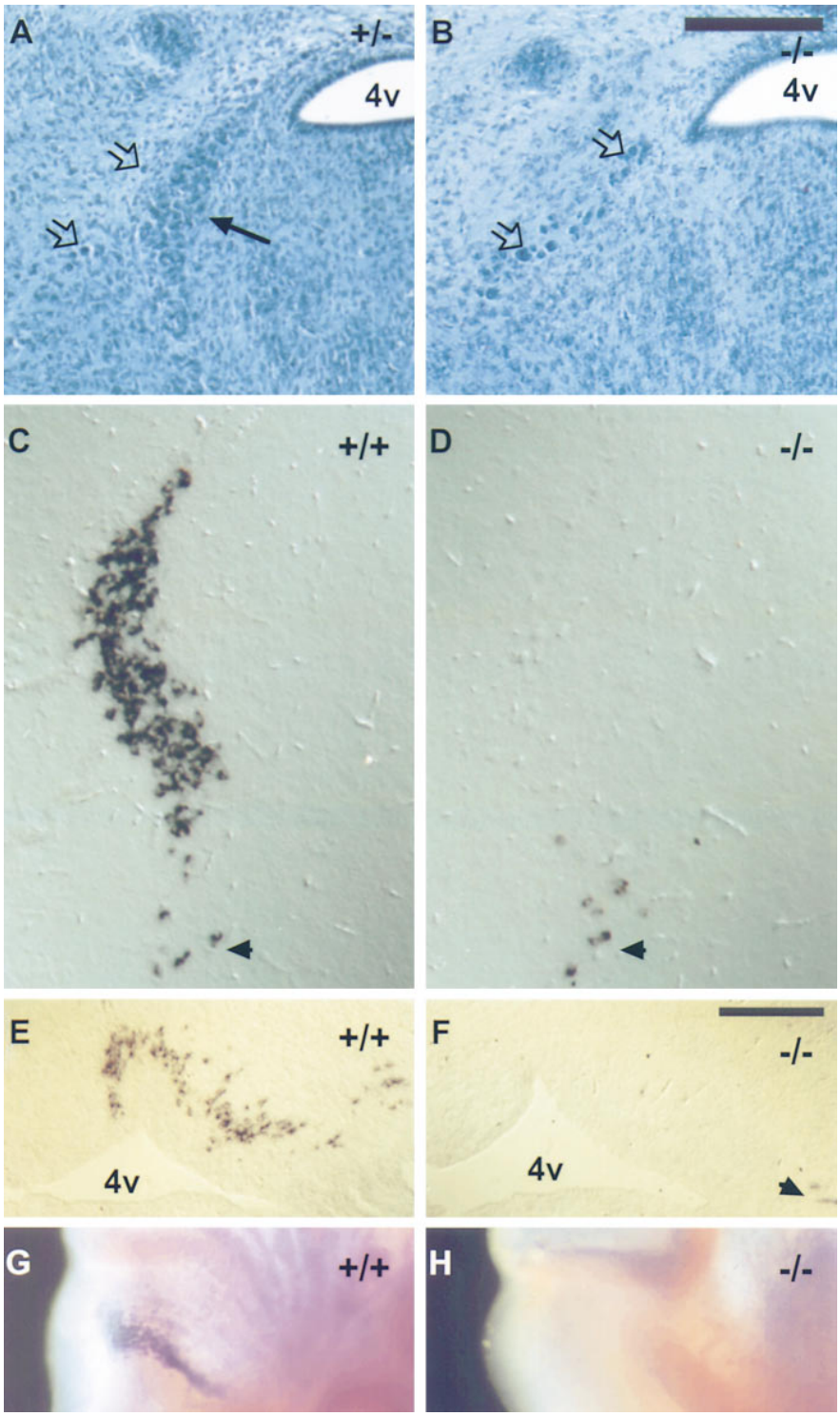

Figure 4. Analysis of the Locus Coeruleus of Wild-Type ([A], [C], [E], and [G]) and mutant ([B], [D], [F], [H]) Mice

(A and B) Histological staining on transverse sections through the rostral pons of neonates. The l.c. is seen as a dense group of cells lateroventral to the fourth ventricle (black arrow) in normal mice (A) and is absent in the mutants (B). The large scattered cells lateral to the normal position of the l.c. seen in mutant and wild-type (open arrows) do not belong to the l.c. as assessed by their lack of expression of DBH (not shown) and probably correspond to the mesencephalic nucleus of the trigeminal nerve.

(C–H) In situ hybridization with a *DBH* antisense RNA probe at different development stages. A transverse section through the pons of neonates shows densely packed DBH^{+} cells in the l.c. of wild-type mice (C), which are not detected in the mutant (D), confirming the absence of a differentiated l.c. in mutant mice at birth. Parasagittal sections of E13.5 embryos ([E] and [F]) and whole-mount preparations at E10.5 ([G] and [H]) also show a strong signal with the *DBH* probe in the l.c. of wild-type embryos ([E] and [G]), whereas no signal is detected in the mutants ([F] and [H]). *DBH*-expressing cells are present in the subcoeruleus area of $Phox2a^{-/-}$ mice (arrowheads in [D] and [F]). 4v, fourth ventricle. Scale bar = 200 μm.

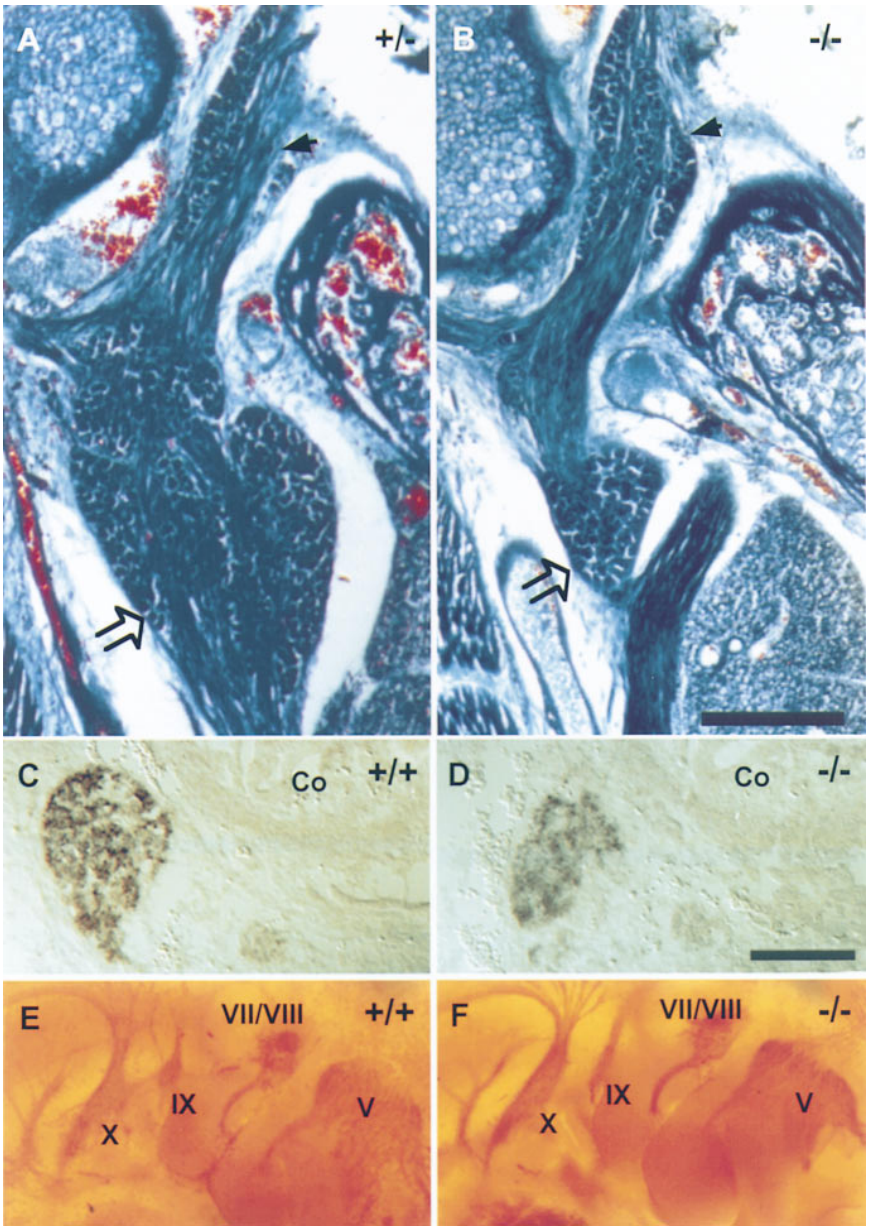

Figure 5. Atrophy of Cranial Sensory Ganglia in *Phox2a*$^{-/-}$ Mice

(A and B) Histological staining on transverse sections at the level of the IXth–Xth cranial sensory ganglia. The petrose–nodose (IXth–Xth distal) complex (open arrows) is dramatically reduced in size in the mutants (F), whereas the jugular–superior (IXth–Xth proximal) complex (arrowheads) is unaffected (see Table 1 for quantitation). (C and D) In situ hybridization with an *Ncam* antisense probe on parasagittal sections through E13.5 embryos shows an atrophy of the IX–Xth distal ganglionic complex in mutant embryos.

(E and F) Whole-mount immunohistochemistry on E10.5 embryos with an antibody directed against a neuron-specific tubulin isoform (TUJ1) shows that the cranial ganglia are not detectably affected at this stage. Co, cochlea; V, IX, and X: ganglia of the Vth, IXth, and Xth cranial nerves; and VII–VIII, VII–VIIIth ganglionic complex. Scale bar = 200 μm.

either *Phox2a*$^{+/+}$ or *Phox2a*$^{-/-}$ were stained for β-galactosidase activity. The VIIth, IXth, and Xth ganglionic anlagen were brightly stained (as well as the trigeminal ganglion) and indistinguishable, with respect to size or signal intensity, in mutant and wild-type embryos, confirming that, at this stage, there is no detectable loss of cells yet (Figures 6D and 6E). Very similar results were obtained by in situ hybridization with a *lacZ* probe (not shown). Therefore, developmental anomalies in these ganglia begin in knockout mice between E10.5 and E13.5.

Altered Gene Expression in *Phox2a*$^{-/-}$ Cranial Ganglia

We made use of the time window during which cranial sensory ganglia are apparently spared to explore possible anomalies in gene expression. The distal IXth and Xth cranial ganglia are known to express noradrenergic

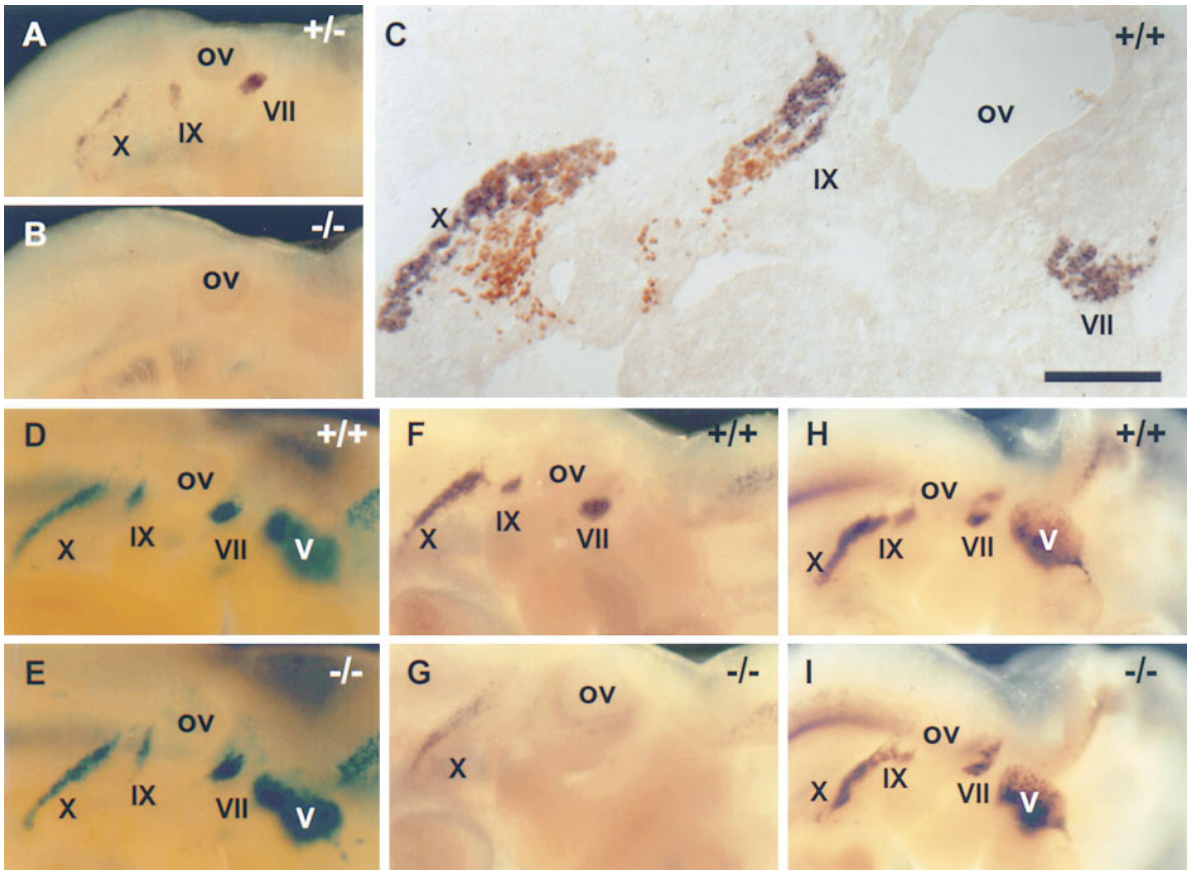

Figure 6. Altered Gene Expression in Early Cranial Sensory Ganglia of *Phox2a*$^{-/-}$ Mice

(A and B) In situ hybridization analysis of *DBH* on whole-mount E9.5 control (A) and mutant (B) embryos. The VIIth ganglion and cells in the forming IXth and Xth ganglion are labeled in wild-type embryos, whereas no signal is detected in mutant littermates.

(C) Double staining with an anti-Phox2a antibody (orange nuclear stain) and a *Ret* antisense riboprobe (purple cytoplasmic stain) on a parasagittal section of an E10.5 control embryo shows Phox2a^{+}/*Ret*$^{-}$ neuroblasts emigrating from the epibranchial placodes. As they aggregate to form the IXth and Xth distal ganglia, they start expressing *Ret*. All cells in the ganglia anlagen appear Phox2a^{+}/*Ret*$^{+}$. On adjacent sections (not shown), the placodes appear Phox2a^{+}. The VIIth ganglion is already formed and entirely double positive.

(D and E) β-galactosidase staining on whole-mount E10.5 embryos harboring the *DBH-LacZ* transgene does not reveal any difference in the size of cranial sensory ganglia between control (D) and *Phox2a*$^{-/-}$ (E) embryos.

(F and G) Whole-mount in situ hybridization on E10.5 embryos shows a dramatic reduction (in the Xth) or disappearance (in the IXth and VIIth) of *Ret*$^{+}$ cells in mutant embryos (G) compared to a wild-type littermate (F).

(H and I) Whole-mount in situ hybridization with a *peripherin* probe on E10.5 embryos shows virtually no difference in the number of cells expressing this neuronal marker between mutant (I) and control (H) ganglia. ov, otic vesicle; and V, VII, IX, X: Vth, VIIth, IXth, and Xth cranial ganglia. Scale bar = 200 μm.

traits as part of their initial differentiation program (Jonakait et al., 1984), thus offering a test of the hypothesized regulatory link between Phox2a and *DBH*. In wild-type embryos, we could indeed detect *DBH* transcripts at E9.5 in the three ganglion anlagen that express Phox2a (Figure 6A). There was a complete loss of *DBH* expression in *Phox2a*$^{-/-}$ mice (Figure 6B), implying that *DBH* is under the direct or indirect control of Phox2a in these ganglia.

It may seem paradoxical, in view of the disappearance of endogenous *DBH* expression, that expression of the *DBH* promoter-*lacZ* transgene was maintained in the mutants. However, as previously reported (Kapur et al., 1991) and amply confirmed by us, the *DBH-lacZ* transgene is ectopically expressed at that stage; in particular, it is expressed at high level in all cranial (including the trigeminal) and spinal sensory ganglia, which contrasts with the low level expression of endogenous *DBH*, confined to the distal VIIth, IXth, and Xth ganglia. A possible explanation is that the Phox2-dependent regulation of the transgene is masked by the effects of a strong Phox2-independent panganglionic enhancer, which is inactive in the context of the endogenous promoter.

We then looked for effects of the *Phox2a* mutation on the receptor tyrosine kinase, *Ret*, whose expression correlates with that of Phox2a in many parts of the peripheral nervous system (Pachnis et al., 1993). In cranial ganglia, *Ret* is expressed early on in the distal placode-derived parts of the VIIth, IXth, and Xth ganglia, precisely those which also express Phox2a (Pachnis et al., 1993; Valarché et al., 1993; Robertson and Mason, 1995; Tiv-

eron et al., 1996). However, Phox2a expression clearly precedes that of *Ret*: it begins in the epibranchial ectodermal placodes and can be followed thereafter in delaminating neuroblasts and the aggregating ganglia anlagen, whereas *Ret* expression is initiated only once the cells coalesce to form the ganglia (Figure 6C). This pattern of *Ret* expression was detectable on whole mounts of E10.5 wild-type embryos (Figure 6F) but was absent (in the VIIth and IXth ganglia) or greatly reduced (in the Xth ganglion) in the mutants (Figure 6G). We conclude that *Ret* expression is directly or indirectly regulated by Phox2a in cranial ganglia.

Finally, we analyzed the expression of the gene encoding the intermediate filament protein peripherin, which is normally expressed in all neurons of the peripheral nervous system (Escurat et al., 1990). Whole-mount preparations of *Phox2a*$^{+/+}$ or *Phox2a*$^{-/-}$ E10.5 embryos were hybridized with a *peripherin* cRNA probe. The anlagen of the VIIth, IXth, and Xth ganglia were readily visible in mutant and wild-type embryos (Figures 6H and 6I).

Therefore, in *Phox2a*$^{-/-}$ mice, the epibranchial placodes give rise to the normal complement of neuroblasts that delaminate and undergo the first phases of "generic" neuronal differentiation, as exemplified by their expression of β-tubulin and peripherin. However, they fail to express part of a more specific differentiation program, including transient expression of *DBH* and expression of *Ret*.

Increased Cell Death in Mutant Cranial Ganglia

Ret has recently been found to be part of the receptor for GDNF (Durbec et al., 1996b; Jing et al., 1996; Treanor et al., 1996; Trupp et al., 1996) on which nodose ganglion neurons depend in vitro (Buj-Bello et al., 1995; Trupp et al., 1995) and in vivo (Moore et al., 1996). We therefore sought to determine whether increased cell death may contribute to the atrophy of the nodose–petrose ganglionic complex, which fails to express *Ret* in the mutants. Parasagittal sections of wild-type or mutant E11.5 embryos were processed for the TUNEL detection method of apoptotic nuclei. Massive apoptotic cell death was apparent in the IXth and Xth distal ganglia from mutants (Figures 7B and 7D), whereas very few, if any, apoptotic nuclei were seen in the controls (Figures 7A and 7C). Therefore, the atrophy of these ganglia can be attributed, at least in part, to an increase in cell death.

Discussion

Phox2a was known to be a marker of two domains of the central and peripheral nervous systems: (nor)adrenergic neurons and the medullary control circuits of autonomic functions (Valarché et al., 1993; Tiveron et al., 1996). By generating a mouse defective for Phox2a, we have demonstrated that this transcription factor is in fact required for the proper development of a subset of these structures: i) the locus coeruleus, the main noradrenergic center of the brain and ii) the parasympathetic ganglia of the head, both absent in the mutants; iii) the cervical sympathetic chain, which has abnormal morphology in the mutants; and iv) the three epibranchial placode-derived cranial ganglia −geniculate, petrose, and nodose−, which are atrophic in the mutants. In cranial ganglia, the existence of a time window before overt degeneration allowed us to explore the role of Phox2a at the molecular level.

Cranial Ganglia Reveal Differentiation Events Controlled by Phox2a

The three cranial sensory ganglia that are part of the visceral nervous system are markedly atrophic in *Phox2a*$^{-/-}$ mice. However, this deficit appears relatively late and is preceded by an ~2 day window where the ontogenesis of these ganglia appears to proceed normally. In particular, even though Phox2a is expressed in the epibranchial placodes from which these ganglia arise, it seems dispensable for the delamination of neuronal progenitors, their aggregation into the ganglionic anlagen, and their expression of some neuronal markers such as β-tubulin and peripherin. However, we could detect two key alterations in gene expression in these forming ganglia. These ganglion cells belong to the class of "transiently catecholaminergic" neurons, which express DBH during development (Jonakait et al., 1984). This expression was abolished in the mutants, providing the first in vivo evidence that Phox2a may regulate neurotransmitter phenotype. The only other transcription factor known to behave as a determinant of neurotransmitter phenotype is another member of the PRX superclass of homeodomain proteins (Bürglin, 1994), Unc30, which controls the GABAergic phenotype in C. elegans (Jin et al., 1994). Strikingly, one other major site affected in *Phox2a* mutants is the l.c., the main noradrenergic center of the brain, although we cannot prove that Phox2a also controls *DBH* in this structure because we cannot detect the cells.

The second marker whose expression is abolished or greatly reduced in these ganglia is the GDNF receptor Ret. GDNF, a member of the TGFβ superfamily, is a survival factor for several classes of neurons in various in vivo and in vitro models (Lin et al., 1993; Henderson et al., 1994; Arenas et al., 1995; Beck et al., 1995; Oppenheim et al., 1995; Yan et al., 1995). GDNF promotes survival of chick nodose neurons in vitro (Buj-Bello et al., 1995; Trupp et al., 1995), and in GDNF-deficient mice produced by gene targeting, the distal IXth and Xth cranial ganglia are atrophic (Moore et al., 1996). Moreover, we show that in *Phox2a*$^{-/-}$ mice, these ganglia undergo a massive increase in apoptosis consistent with their having lost the capacity to respond to a survival factor. Taken together, these data argue that it is through the regulation of *Ret* expression that Phox2a exerts its trophic control on these cranial ganglia. It will be important to examine *Ret* knockout mice (Schuchardt et al., 1994) for a similar deficit in these ganglia. Obviously, not all ganglion cells are affected, and it remains unresolved whether the neurons that are impervious to the *GDNF* or *Phox2a* mutations represent a random sample or a defined subpopulation. The disappearance of the l.c. cannot be attributed to the same mechanism because it does not express *Ret* until at least E13.5 (not shown) and, accordingly, is spared in *GDNF* knockout mice (Moore et al., 1996; Sánchez et al., 1996).

Phox2a^{+} structures other than cranial ganglia and the

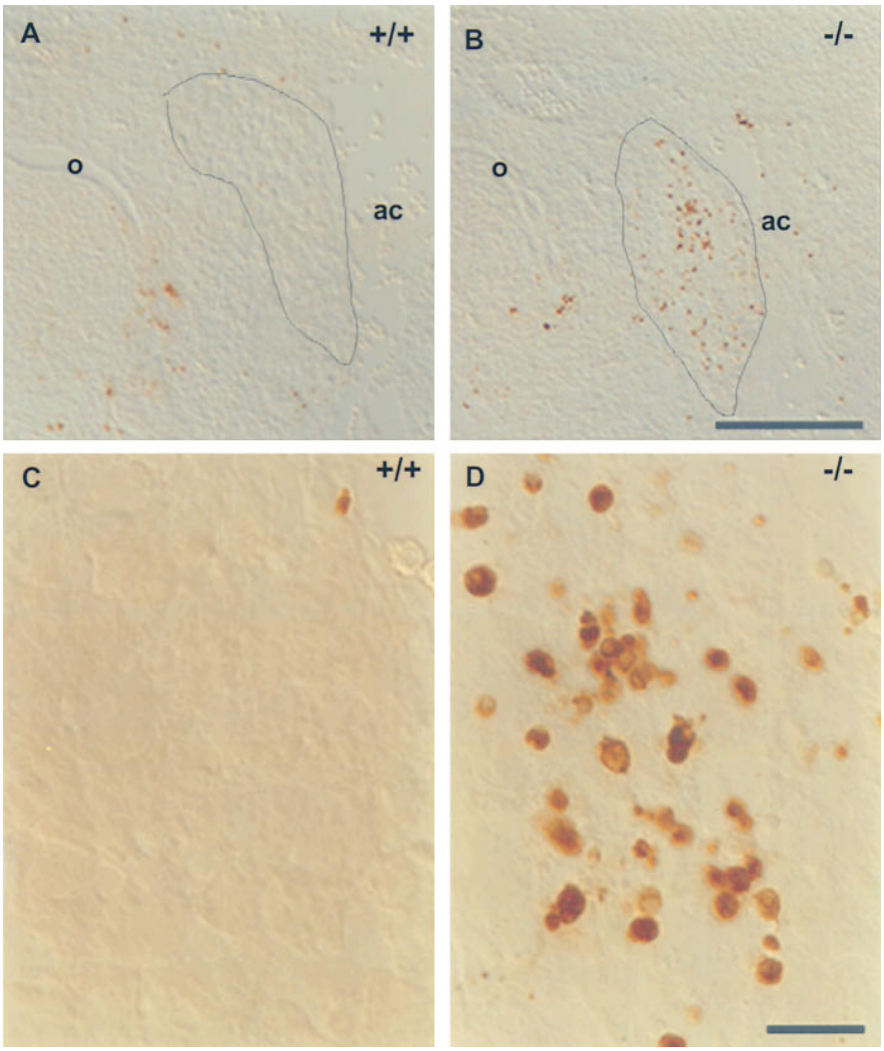

Figure 7. Apoptosis in the Cranial Ganglia of E11.5 *Phox2a*$^{-/-}$ Mice

(A and B) Parasagittal sections through E11.5 embryos labeled with the TUNEL method for detection of apoptotic cells: massive apoptosis is detectable in the petrose–nodose complex of mutant embryos (B), whereas virtually no cells are labeled in the control. The ganglion outline, determined by in situ hybridization with a *peripherin* probe on adjacent sections (not shown), is indicated.

(C and D) Higher magnification of the same sections. ac, anterior cardinal vein; and o, oropharynx. Scale bars = 200 μm, (A) and (B); 20 μm, (C) and (D).

l.c. express *DBH* (sympathetic ganglia; enteric neuroblasts; and noradrenergic centers A1, A2, and A5) or *Ret* (sympathetic ganglia, enteric neuroblasts, some parasympathetic ganglia, and the facial nucleus) and maintain that expression in the mutants. Remarkably, these structures also retain *Phox2b* expression in the mutants, which is compatible with a functional redundancy between the two genes in the control of *Ret* and *DBH* (A. Pattyn, X. M., C. G., and J.-F. B., unpublished data).

Phox2a and the Control of Neuronal Identity

In vertebrates, changing the expression of transcription factors does not always reveal their exact role in controlling cell phenotypes, since the consequence of knockout experiments, if any, is often the loss of those cells that express the factor. It is therefore difficult to uncouple the phenotypes of cells from their very existence. In this context, it is remarkable that we found Phox2a to coregulate a conventional differentiation trait–a neurotransmitter biosynthesis enzyme–and a receptor for a survival factor. How direct these regulations are remains to be determined. A high affinity binding site for Phox2a was found in the *DBH* promoter (Tissier-Seta et al., 1993), and moderate transactivaton of *DBH* promoter activity by Phox2a has been reported in transient transfection experiments (Zellmer et al., 1995). No data are currently available on the *Ret* promoter. Therefore, it is still possible that the coregulation of *DBH* and *Ret* is indirect and through different transcriptional cascades.

Whether direct or indirect, this coregulation could, if it is generalizable to other neuronal types, provide a simple mechanism for the tight link between neuronal

identity and survival that one can infer from many transcription factor knockout experiments. The biological relevance of such a link may lie in the fact that it ensures that only neurons that have engaged in the differentiation program appropriate for a given location and developmental stage can survive.

In contrast to *DBH* and *Ret*, the expression of the general neuronal markers β-tubulin and *peripherin* was not affected by the mutation. This argues that induction of a "generic" neuronal phenotype and of a neuronal-type specific differentiation program are controlled independently. In an analogous fashion, notochord ablation experiments have shown that in sympathetic precursor cells, induction of the more general neuronal markers SCG10 and Cash-1 can be uncoupled from the induction of *Phox2a* and *TH* (Groves et al., 1995).

It is striking that, whereas some Phox2a-expressing neurons are severely affected by the *Phox2a* mutation, others are not, with no readily apparent logic. One classic explanation for this type of finding is redundancy of function with another coexpressed molecule. The closely related Phox2b protein is a good candidate for compensating for the loss of Phox2a in certain cell types. Indeed, all cell types unaffected in *Phox2a*$^{-/-}$ mice, either morphologically or in their expression of *DBH* or *Ret*, retain expression of *Phox2b* in the mutants (A. Pattyn, X. M., C. G., and J.-F. B., unpublished data). This raises the possibility that "Phox2 function" is ensured by at least two proteins, and its extent is only partially revealed by the knockout of the *Phox2a* gene.

Experimental Procedures

Construction of a Phox2a Targeting Vector

A clone (pG2.3) containing the entire *Phox2a* gene was isolated from a mouse C57BL/6J phage genomic library by hybridization with a 380 bp EcoRI-NruI 5′ *Phox2a* cDNA fragment from clone pab903 (Valarché et al., 1993). To generate the targeting construct (pΔPhox2a), we first constructed a vector (pKO) containing a *neo*-resistance gene derived from the pMC1NeoPolyA vector (Mansour et al., 1988) flanked in 5′ with a multiple cloning site and separated in 3′ from the HSV-*tk* cassette by a BamHI site. A 9 kb BamHI 3′ fragment of the *Phox2a* gene was inserted between the *neo* and HSV-*tk* genes of pKO and the short arm by inserting a PCR-generated 1.25 kb 5′ fragment into the NotI and SpeI sites 5′ to the *neo* gene. For optimization and control of PCR analysis of recombination events, a control plasmid was generated by insertion, instead of the 1.25 kb short arm, of a 1.33 kb PCR fragment, 80 bp longer on the 5′ side.

ES Cell Culture

The ES cell line E14–1 was cultured on mitomycine C-inactivated, G418-resistant primary mouse embryonic fibroblasts. ES cells (10^7) were transfected by electroporation (BioRad Gene Pulser; 240 V; 500 μF) with 25 μg of targeting construct linearized with NotI. Selection with 350 μg/ml G418 (GIBCO BRL) and 2 μM gancyclovir (Cymevan; Syntex Laboratories) was applied. Double-resistant colonies were picked on days 11–13. Half of each colony was lysed for PCR analysis, and the other half was seeded on 96-well plates and further cultured. Colonies from PCR-positive pools were passaged on 24-well plates and individually tested by PCR. PCR-positive clones were then frozen and expanded for Southern blot analysis.

PCR Screening of Recombinant Clones and Southern Blot Analysis

Double-resistant colonies were screened in pools of eight. After proteinase K treatment, samples were subjected to PCR using standard conditions. Primers, amplifying a 1.45 kb fragment, were derived from *Phox2a* genomic sequences in intron 1 (5′-ATGCCTTCTG TTAGTGTCCCAGCAT-3′) and from the *neo* cassette (5′-TCGACATT GGGTGGAAACATTCCAG-3′). G418-resistant ES cells transfected with the control plasmid were used as a positive control for the PCR analysis. DNA of PCR-positive clones was isolated (adapted from Miller et al., 1988) and digested with SstI or XbaI, transferred by Southern blotting on Hybond N membranes (Amersham) and hybridized to an external 5′ probe (1 kb SstI-XhoI fragment containing part of exon 1 and intron 1) and a *neo* probe (1,1 kb SpeI-BamHI fragment). We obtained a total of nine correctly targeted lines from 333 double-resistant clones.

Generation of Chimeras and Mating of Mice

Recombinant ES cells were injected into C57/BL6 blastocysts. Male chimeras were bred to C57/BL6 females. Germ line transmission was obtained for two of four injected ES cell lines. Heterozygous (C57/BL6 × 129) offspring were interbred to produce homozygous animals. F2 animals were genotyped either by Southern blot analysis using the 5′ external probe on DNA from tail or extraembryonic membranes (Laird et al., 1991) or by PCR analysis on DNA obtained from embryonic tail or rear limb (Blaugrund et al., 1996) using two pairs of primers: one pair, located within the *neo* gene (5′-TTTGTC AAGACCGACCTGTC-3′; 5′-CGATACCGTAAAGCACGAGG-3′) reveals a 598 bp fragment in the mutated allele; the other pair, located within the deleted region (5′-CTGCATGAGAAGCGCAAGCA-3′, 5′-TTAGCAAGCGGTGCACAGCA-3′) reveals a 190 bp band in the wild-type allele.

Generation of *Phox2a*$^{-/-}$, *DBH-LacZ* Mice

Mice heterozygous for the *Phox2a* mutation and hemizygous for the *DBH-LacZ* transgene (Kapur et al., 1991) were obtained by breeding *Phox2a*$^{+/-}$ F1 females with a homozygous *DBH-LacZ* male. These mice were genotyped by dot blot analysis using *neo* and *lacZ* probes and interbred to produce *Phox2a*$^{-/-}$, *DBH-LacZ* mice (3/16 embryos). Embryos resulting from these crosses were genotyped by PCR and staining for galactosidase activity (Knittel et al., 1995).

Histology

Newborn mice were given an overdose of anesthetic, skinned, fixed in Bouin's solution (Sigma) for several days, decalcified, dehydrated, and embedded in paraffin wax. Transverse and parasagittal sections of the head and neck were cut at 12 μm and stained with Groat's hematoxylin and Mallory's trichrome (Mark et al., 1993).

The total number of neurons in cranial ganglia was counted using a protocol adapted from Piñón et al. (1996). The ganglionic profile of every fifth section was drawn–excluding the areas containing only fibers–and its surface was measured using an image analysis program (Optimas). The average neuron density in each section was quantified by counting all neurons having a clear nucleus in a defined area (2750 μm^2 for the geniculate ganglion; 6950 μm^2 for all the others). The total cross-sectional area of the ganglion was calculated by adding the section areas and multiplying by 5. The total number of neurons in the ganglion was calculated from this value and the average neuron density (the neuron density did not differ significantly from one section to another in a given individual but differed between individuals).

In Situ Hybridization and Immunohistochemistry

Nonradioactive antisense RNA probes for *DBH*, *TH*, *Ncam*, *peripherin*, and *Ret* were labeled using the DIG RNA labeling kit (Boehringer Mannheim), following the manufacturer's instructions. In situ hybridization and immunohistochemistry on sections as well as whole-mount in situ hybridization were performed as described by Tiveron et al. (1996). Whole-mount immunohistochemistry was performed according to Lee et al. (1995).

Neurons undergoing apoptotic cell death in the petrose and nodose ganglia were detected by the TUNEL method, using the ApopTag detection kit (Oncor).

Acknowledgments

We thank M.-C. Tiveron for contributing the *c-ret*/Phox2a double-labeling experiment, V. Pachnis for the *c-ret* probe, M.-M. Portier for the *peripherin* probe, K. Rajewsky for the E14–1 cell line and

the *tk-neo* cassette, and C. Henderson for critical reading of the manuscript. This work was supported by institutional grants from CNRS and Université de la Méditerranée, by a European Community fellowship for H. C., and by specific grants from Ministère de l'Enseignement Supérieur et de la Recherche (ACC-SV4), European Community Biomed program (grant BMH4-CT95–0524), Association Française contre les Myopathies, and Association pour la Recherche sur le Cancer.

Received December 9, 1996; revised February 19, 1997.

References

Appel, B., Korzh, V., Glasgow, E., Thor, S., Edlund, T., and Dawid, I.B. (1995). Motoneuron fate specification revealed by patterned LIM homeobox gene expression in embryonic zebrafish. Development *121*, 4117–4125.

Arenas, E., Trupp, M., Åkerud, P., and Ibáñez, C.F. (1995). GDNF prevents degeneration and promotes the phenotype of brain noradrenergic neurons in vivo. Neuron *15*, 1465–1473.

Bang, A.G., and Goulding, M.D. (1996). Regulation of vertebral neural cell fate by transcription factors. Curr. Opin. Neurobiol. *6*, 25–32.

Beck, K.D., Valverde, J., Alexi, T., Poulsen, K., Moffat, B., Vandlen, R.A., Rosenthal, A., and Hefti, F. (1995). Mesencephalic dopaminergic neurons protected by GDNF from axotomy-induced degeneration in the adult brain. Nature *373*, 339–341.

Blaugrund, E., Pham, T.D., Tennyson, V.M., Lo, L., Sommer, L., Anderson, D.J., and Gershon, M.D. (1996). Distinct subpopulations of enteric neuronal progenitors defined by time of development, sympathoadrenal lineage markers and *Mash-1*-dependence. Development *122*, 309–320.

Buj-Bello, A., Buchman, V.L., Horton, A., Rosenthal, A., and Davies, A.M. (1995). GDNF is an age-specific survival factor for sensory and autonomic neurons. Neuron *15*, 821–828.

Bürglin, T.R. (1994). A comprehensive classification of homeobox genes. In Guidebook to the Homeobox Genes, D. Duboule, ed. (Oxford: Oxford University Press), pp. 25–71.

Durbec, P.L., Larsson-Blomberg, L.B., Schuchardt, A., Costantini, F., and Pachnis, V. (1996a). Common origin and developmental dependence on *c-ret* of subsets of enteric and sympathetic neuroblasts. Development *122*, 349–358.

Durbec, P., Marcos-Gutierrez, C.V., Kilkenny, C., Grigoriou, M., Wartiowaara, K., Suvanto, P., Smith, D., Ponder, B., Costantini, F., Saarma, M., Sariola, H., Pachnis, V. (1996b). GDNF signalling through the Ret receptor tyrosine kinase. Nature *381*, 789–793.

Easter, S.S., Jr., Ross, L.S., and Frankfurter, A. (1993). Initial tract formation in the mouse brain. J. Neurosci. *13*, 285–299.

Erkman, L., McEvilly, R.J., Luo, L., Ryan, A.K., Hooshmand, F., O'Connell, S.M., Keithley, E.M., Rapaport, D.H., Ryan, A.F., and Rosenfeld, M.G. (1996). Role of transcription factors Brn-3.1 and Brn-3.2 in auditory and visual system development. Nature *381*, 603–606.

Ernsberger, U., Patzke, H., Tissier-Seta, J.-P., Reh, T., Goridis, C., and Rohrer, H. (1995). The expression of tyrosine hydroxylase and the transcription factors cPhox-2 and Cash-1: evidence for distinct inductive steps in the differentiation of chick sympathetic precursor cells. Mech. Dev. *52*, 125–136.

Escurat, M., Djabali, K., Gumpel, M., Gros, F., and Portier, M-M. (1990). Differential expression of two neuronal intermediate-filament proteins, peripherin and the low-molecular-mass neurofilament (NF-L), during the development of the rat. J. Neurosci. *10*, 764–784.

Gan, L., Xiang, M., Zhou, L., Wagner, D.S., Klein, W.H., and Nathans, J. (1996). POU domain factor Brn-3b is required for the development of a large set of retinal ganglion cells. Proc. Natl. Acad. USA *93*, 3920–3925.

Ghysen, A., and Dambly-Chaudière, C. (1993). The specification of sensory neuron identity in *Drosophila*. Bioessays *15*, 293–298.

Goddard, J.M., Rossel, M., Manley, N.R., and Capecchi, M.R. (1996). Mice with targeted disruption of *Hoxb-1* fail to form the motor nucleus of the VIIth nerve. Development *122*, 3217–3228.

Groves, A.K., George, K.M., Tissier-Seta, J.-P., Engel, J.D., Brunet, J.-F., and Anderson, D.J. (1995). Differential regulation of transcription factor gene expression and phenotypic markers in developing sympathetic neurons. Genes Dev. *121*, 887–901.

Henderson, C.E., Phillips, H.S., Pollock, R.A., Davies, A.M., Lemeulle, C., Armanini, M., Simmons, L., Moffet, B., Vandlen, R.A., Koliatsos, V.E., and Rosenthal, A. (1994). GDNF: a potent survival factor for motoneurons present in peripheral nerve and muscle. Science *266*, 1602–1604.

Higashijima, S-i., Michiue, T., Emori, Y., and Saigo, K. (1992). Subtype determination of *Drosophila* embryonic external sensory organs by redundant homeo box genes *BarH1* and *BarH2*. Genes Dev. *6*, 1005–1018.

Jin, Y., Hoskins, R., and Horvitz, H.R. (1994). Control of type-D GABAergic neuron differentiation by C. elegans UNC-30 homeodomain protein. Nature *372*, 780–783.

Jing, S., Wen, D., Yu, Y., Holst, P.L., Luo, Y., Fang, M., Tamir, R., Antonio, L., Hu, Z., Cupples, R., Louis, J-C., Hu, S., Altrock, B.W., and Fox, G.M. (1996). GDNF-induced activation of the Ret protein tyrosine kinase is mediated by GDNFR-α, a novel receptor for GDNF. Cell *85*, 1113–1124.

Jonakait, G.M., Markey, K.A., Goldstein, M., and Black, I.B. (1984). Transient expression of selected catecholaminergic traits in cranial sensory and dorsal root ganglia of the embryonic rat. Dev. Biol. *101*, 51–60.

Kapur, R.P., Hoyle, G.W., Mercer, E.H., Brinster, R.L., and Palmiter, R.D. (1991). Some neuronal cell populations express human dopamine β-hydroxylase-lacZ transgenes transiently during embryonic development. Neuron *7*, 717–727.

Kimura, S., Hara, Y., Pineau, T., Fernandez-Salguero, P., Fox, C.H., Ward, J.M., and Gonzalez, F.J. (1996). The T/ebp null mouse: thyroid-specific enhancer-binding protein is essential for the organogenesis of the thyroid, lung, ventral forebrain, and pituitary. Genes Dev. *10*, 60–69.

Knittel, T., Kessel, M., Kim, M.H., and Gruss, P. (1995). A conserved enhancer of the human and murine *Hoxa-7* gene specifies the anterior boundary of expression during embryonal development. Development *121*, 1077–1088.

Laird, P.W., Zijderveld, A., Linders, K., Rudnicki, M.A., Jaenisch, R., and Berns, A. (1991). Simplified mammalian DNA isolation procedure. Nucleic Acids Res. *19*, 4293.

Lee, K.-F., Simon, H., Chen, H., Bates, B., Hung, M.-C., and Hauser, C. (1995). Requirement for neuregulin receptor erbB2 in neural and cardiac development. Nature *378*, 394–398.

Lin, L.F., Doherty, D.H., Lile, J.D., Bektesh, S., and Collins, F. (1993). GDNF: a glial cell line–derived neurotrophic factor for midbrain dopaminergic neurons. Science *260*, 1130–1132.

Mansour, S.L., Thomas, K.R., and Capecchi, M.R. (1988). Disruption of the proto-oncogene *int-2* in mouse embryo-derived stem cells: a general strategy for targeting mutations to non-selectable genes. Nature *336*, 348–352.

Mark, M., Lufkin, T., Vonesch, J.-L., Ruberte, E., Olivo, J.-C., Dollé, P., Gorry, P., Lumsden, A., and Chambon, P. (1993). Two rhombomeres are altered in *Hoxa-1* mutant mice. Development *119*, 319–338.

Mercer, E.H., Hoyle, G.W., Kapur, R.P., Brinster, R.L., and Palmiter, R.D. (1991). The dopamine beta-hydroxylase gene promoter directs expression of E. coli *lacZ* to sympathetic and other neurons in adult transgenic mice. Neuron *7*, 703–716.

Miller, D.M., III, and Niemeyer, C.J. (1995). Expression of the Unc-4 homeoprotein in Caenorhabditis elegans motor neurons specifies presynaptic input. Development *121*, 2877–2886.

Miller, S.A., Dykes, D.D., and Polesky, H.F. (1988). A simple salting out procedure for extracting DNA from human nucleated cells. Nucleic Acids Res. *16*, 1215.

Miller, D.M., Shen, M.M., Shamu, C.E., Bürglin, T.R., Ruvkun, G., Dubois, M.L., Ghee, M., and Wilson, L. (1992). *C. elegans unc-4 gene* encodes a homeodomain protein that determines the pattern of synaptic input to specific neurons. Nature *355*, 841–845.

Moore, M.W., Klein, R.D., Fariñas, I., Sauer, H., Armanini, M., Phillips, H., Reichardt, L.F., Ryan, A.M., Carver-Moore, K., and Rosenthal, A. (1996). Renal and neuronal abnormalities in mice lacking GDNF. Nature *382*, 76–79.

Nakai, S., Kawano, H., Yudate, T., Nishi, M., Kuno, J., Nagata, A., Jishage, K-i., Hamada, H., Fujii, H., Kawamura, K., Shiba, K., and Noda, T. (1995). The POU domain transcription factor Brn-2 is required for the determination of specific neuronal lineages in the hypothalamus of the mouse. Genes Dev. *9*, 3109–3121.

Oppenheim, R.W., Houenou, L.J., Johnson, J.E., Lin, L.-F. H., Li, L., Lo, A.C., Newsome, A.L., Prevette, D.M., and Wang, S. (1995). Developing motor neurons rescued from programmed and axotomy-induced cell death by GDNF. Nature *373*, 344–346.

Pachnis, V., Mankoo, B., and Costantini, F. (1993). Expression of the *c-ret* proto-oncogene during mouse embryogenesis. Development *119*, 1005–1017.

Pfaff, S.L., Mendelsohn, M., Stewart, C.L., Edlund, T., and Jessell, T.M. (1996). Requirement for LIM homeobox gene *Isl1* in motor neuron generation reveals a motor neuron-dependent step in interneuron differentiation. Cell *84*, 309–320.

Piñón, L.G.P., Minichiello, L., Klein, R., and Davies, A.M. (1996). Timing of neuronal death in *trkA*, *trkB*, and *trkC* mutant embryos reveals developmental changes in sensory neuron dependance on Trk signaling. Development *122*, 3255–3261.

Robertson, K., and Mason, I. (1995). Expression of *ret* in the chicken embryo suggests roles in regionalisation of the vagal neural tube and somites and in development of multiple neural crest and placodal lineages. Mech. Dev. *53*, 329–344.

Rubenstein, J.L.R., and Puelles, L. (1994). Homeobox gene expression during development of the vertebrate brain. Curr. Top. Dev. Biol. *30*, 2–63.

Rubin, E. (1985). Development of the rat superior cervical ganglion: ganglion cell maturation. J. Neurosci. *5*, 673–684.

Sánchez, M.P., Silos-Santiago, I., Frisén, J., He, B., Lira, S.A., and Barbacid, M. (1996). Renal agenesis and the absence of enteric neurons in mice lacking GDNF. Nature *382*, 70–73.

Schonemann, M.D., Ryan, A., McEvilly, R.J., O'Connell, S.M., Arias, C.A., Kalla, K.A., Li, P., Sawchenko, P.E., and Rosenfeld, M.G. (1995). Development and survival of the endocrine hypothalamus and posterior pituitary gland requires the neuronal POU domain factor Brn-2. Genes Dev. *9*, 3122–3135.

Schuchardt, A., D'Agati, V., Larsson-Blomberg, L., Costantini, F., and Pachnis, V. (1994). Defects in the kidney and enteric nervous system of mice lacking the tyrosine kinase receptor Ret. Nature *367*, 380–383.

Tissier-Seta, J.-P., Hirsch, M.-R., Valarché, I., Brunet, J.-F., and Goridis, C. (1993). A possible link between cell adhesion receptors, homeodomain proteins and neuronal identity. C. R. Acad. Sci. (Paris) *316*, 1305–1315.

Tiveron, M.-C., Hirsch, M.-R., and Brunet, J.-F. (1996). The expression pattern of the transcription factor Phox2a delineates synaptic pathways of the autonomic nervous system. J. Neurosci. *16*, 7649–7660

Treanor, J.J.S., Goodman, L., de Sauvage, F., Stone, D.M., Poulsen, K.T., Beck, C.D., Gray, C., Armanini, M.P., Pollock, R.A., Hefti, F., Phillips, H.S., Goddard, A., Moore, M.W., Buj-Bello, A., Davies, A.M., Asai, N., Takahashi, M., Vandlen, R., Henderson, C.E., and Rosenthal, A. (1996). Characterization of a multicomponent receptor for GDNF. Nature *382*, 80–83.

Trupp, M., Rydén, M., Jörnvall, H., Funakoshi, H., Timmusk, T., Arenas, E., and Ibáñez, C.F. (1995). Peripheral expression and biological activities of GDNF, a new neurotrophic factor for avian and mammalian peripheral neurons. J. Cell Biol. *130*, 137–148.

Trupp, M., Arenas, E., Fainzilber, M., Nilsson, A.-S., Sieber, B.-A., Grigoriou, M., Kilkenny, C., Salazar-Grueso, E., Pachnis, V., Arumäe, U., Sariola, H., Saarma, M., and Ibáñez, C.F. (1996). Functional receptor for GDNF encoded by the c-*ret* proto-oncogene. Nature *381*, 785–789.

Tsuchida, T., Ensini, M., Morton, S.B., Baldassare, M., Edlund, T., Jessell, T.M., and Pfaff, S.L. (1994). Topographic organization of embryonic motor neurons defined by expression of LIM homeobox genes. Cell *79*, 957–970.

Valarché, I., Tissier-Seta, J.-P., Hirsch, M.-R., Martinez, S., Goridis, C., and Brunet, J.-F. (1993). The mouse homeodomain protein Phox2a regulates *Ncam* promoter activity in concert with Cux/CDP and is a putative determinant of neurotransmitter phenotype. Development *119*, 881–896.

Yan, Q., Matheson, C., and Lopez, O.T. (1995). *In vivo* neurotrophic effects of GDNF on neonatal and adult facial motor neurons. Nature *373*, 341–344.

Zellmer, E., Zhang, Z., Greco, D., Rhodes, J., Cassel, S., and Lewis, E.J. (1995). A homeodomain protein selectively expressed in noradrenergic tissue regulates transcription of neurotransmitter biosynthetic genes. J. Neurosci. *15*, 8109–8120.